Negative-Bias Light Stress Instability Mechanisms of the Oxide-Semiconductor Thin-Film Transistors Using In–Ga–O Channel Layers Deposited With Different Oxygen Partial Pressures

Jun Yong Bak, Shinhyuk Yang, Ho-Jun Ryu, Sang Hee Ko Park, Chi Sun Hwang, and Sung Min Yoon

***Abstract*— An In–Ga–O (IGO) semiconductor was employed as a channel layer for the oxide thin-film transistors (TFTs). The IGO composition was chosen as an In/Ga atomic ratio of 65/35 and the films were deposited by RF magnetron sputtering method. To investigate the negative-bias illumination stress (NBIS) instability mechanisms, the IGO films were prepared with various oxygen partial pressures (O_2/Ar+O_2 and P_{O2}). The saturation mobilities of TFTs decreased with increasing P_{O2}, which suggested that the increase in P_{O2} reduced the carrier concentration. The NBIS characteristics of the TFTs were evaluated with the amounts of negative shifts in turn-on voltages (ΔV_{ON}) under the illumination of typical red, green, and blue wavelengths with a V_{GS} of −20 V for 10^4 s. The X-ray photoelectron spectroscopy analysis strongly suggested that the ΔV_{ON} could be caused by the weakening of bonding strength between the atoms, which were analyzed as variations in the red shifts of O 1s peak. The drastic increase in the ΔV_{ON} of the TFT using the IGO prepared without oxygen under the NBIS using the blue illumination was well explained by the combination defect model composed of intrinsic and extrinsic defects inherent within the IGO channel layer.**

***Index Terms*— In–Ga–O (IGO), light instability, oxide semiconductor, RGB light.**

I. Introduction

OXIDE-SEMICONDUCTOR based thin-film transistors (TFTs) have extensively been researched in recent years due to their outstanding characteristics such as high mobility, low-temperature process compatibility, and uniform device performance for the backplanes of flat-panel displays [1], [2]. There are a few important factors affecting the performance of oxide TFT, such as device structure, fabrication methods, employed materials, and their semiconducting layer has a significant impact on not only deposition conditions. Especially, the composition of oxide such electrical parameters as a field-effect mobility (μ_{FE}), a threshold voltage (V_{TH}), a subthreshold swing (SS), and an ON/OFF current ratio ($I_{ON/OFF}$) but also a required temperature to optimize the device performances [3], because of these significant effects, lots of oxide channel materials such as In–Zn–O [3], In–Ga–Zn–O (IGZO) [4], [5], Zn–In–Sn–O [6], and Al–In–Zn–Sn–O [7] have been proposed as a semiconducting layer for the oxide TFTs. Recently, because the mobility needs to be enhanced to realize the ultradefinition display applications, In-rich In–Ga–O (IGO) composition has recently been adopted as one of the promising channel materials to provide high-mobility backplane devices for the next generation displays such as 4K2K liquid crystal display panels and 3-D displays. While intrinsic oxygen deficiency in the In_2O_3 can lead to the performance of high mobility, undesirable negative shift in the threshold voltage with increasing the oxygen vacancies may cause some detrimental problems [8], [9]. These effects for various channel materials can be controlled by incorporating such atoms as gallium (Ga), hafnium (Hf), and silicon (Si) [10]–[12]. Similarly, the In_2O_3 incorporated with suitable amounts of Ga can be expected to be one of the promising solutions to obtain both characteristics of high mobility and operational stability. Ebata *et al.* [13] reported the IGO TFTs using the crystalline In_2O_3 with bixbyite structure as a channel layer, in which a high carrier mobility of 39.1 $cm^2\ V^{-1}\ s^{-1}$ was successfully obtained owing to the crystalline phase with high In contents and large grain size. In addition, the effects of oxygen partial pressure during the IGO deposition on the TFT behaviors were investigated, in which the saturation mobility was obtained to be approximately 43 $cm^2\ V^{-1}\ s^{-1}$ even after the relatively low temperature annealing process of 150 °C [15]. With all these efforts for development of high-mobility IGO TFTs, the studies on the operational instabilities under various circumstances are not enough to guarantee the suitability of IGO as an optimized channel material for the oxide TFT. It is very important for the oxide TFTs with higher carrier mobility to be guaranteed in viewpoints of device stabilities and reliabilities. The stability characteristics under various stress conditions such as positive or negative gate-bias stress (NBS) at higher temperature and/or light illumination

Manuscript received July 8, 2013; revised October 22, 2013; accepted October 25, 2013. Date of current version December 20, 2013. This work was supported in part by the National Research Foundation of Korea funded by the Korea Government under Grant 2012011730, in part by the Basic Science Research Program of the National Research Foundation of Korea funded by the Ministry of Education, Science and Technology under Grant 2011-0008716, and in part by the Ministry of Science, ICT and Future Planning, Korea in the ICT Research and Development Program 2013. The review of this paper was arranged by Editor E. Rosenbaum.

J. Y. Bak and S. M. Yoon are with the Department of Advanced Materials Engineering for Information and Electronics, Kyung-Hee University, Yongin 446-701, Korea (e-mail: sungmin@khu.ac.kr).

S. Yang, H.-J. Ryu, S. H. K. Park, and C. S. Hwang are with the Electronics and Telecommunications Research Institute, Daejeon 305-350, Korea.

Color versions of one or more of the figures in this paper are available online at http://ieeexplore.ieee.org.

Digital Object Identifier 10.1109/TED.2013.2288264

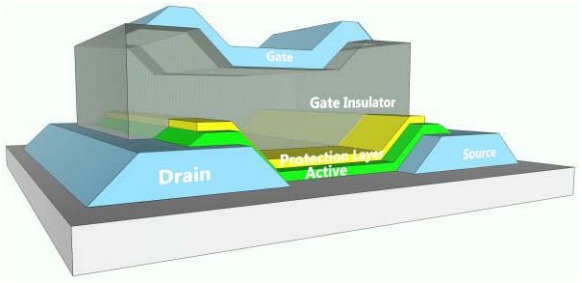

Fig. 1. Schematic diagram of fabricated IGO TFTs with top-gate bottom-contact structure.

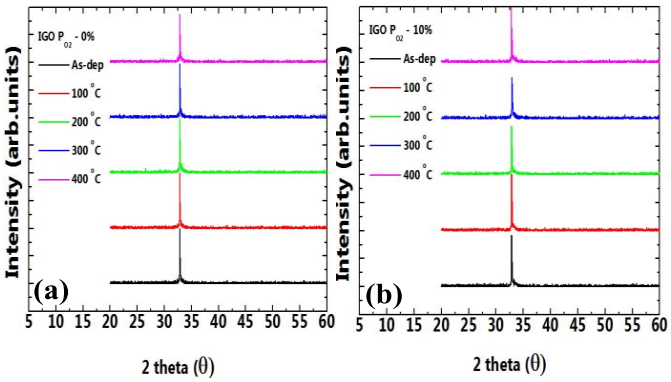

Fig. 2. XRD patterns of the IGO thin films deposited on Si substrate with the PO2 conditions of (a) 0% and (b) 10%. The prepared films were thermally annealed at 100 °C, 200 °C, 300 °C, and 400 °C in a vacuum. The diffraction patterns were measured by using Cu-Kα radiation (40 kV/60 mA) at a scan rate of 3°/min.

stress become critical matters of concerns in realizing not only a large-sized and high-resolution display panels but also a future displays such as transparent and curved panels operated by oxide TFT backplanes. Especially, some kinds of day light effect cannot be avoidable because of the optical transparency of oxide semiconducting channel layer having a wide bandgap. However, for the IGO TFTs with a higher mobility, there have hardly been reports on the device behaviors and their variations under light illumination stress conditions. In addition, the effects of oxygen partial pressure during the channel layer deposition on the instability of oxide TFT under the gate-bias light illumination stress were also barely investigated.

In this paper, we fabricated the TFTs by using the IGO thin films with as oxide channel layers to investigate the relationships between the device characteristics including the stabilities and the IGO deposition conditions of oxygen partial pressure ($P_{O2} = O_2/Ar+O_2$) controlled to be 0%, 5%, 10%, and 15%. In this paper, the composition of IGO with In/Ga atomic ratio of 65/35 was carefully chosen to obtain both performances of high mobility and excellent stability. In addition, as the effective means to elucidate the mechanisms of the instabilities under negative-bias illumination stress (NBIS), the transfer characteristics of the fabricated IGO TFTs were systematically evaluated with changing the wavelength (red, green, and blue) of the illuminated light sources. From these in-depth studies on the NBIS characteristics for the IGO TFTs, we could deduce significantly important conclusions to optimize the deposition conditions for the IGO channels and enhance the overall performances of the IGO TFTs.

II. Experiment

We have fabricated the IGO TFTs with top-gate bottom-contact structure on a glass substrate, as show in Fig. 1. A 150-nm-thick ITO source/drain (S/D) electrodes were deposited by dc sputtering method at room temperature. The ITO was annealed at 200 °C in a vacuum to obtain a better electrical conductivity. After patterning process for the formation of S/D regions, a 20-nm-thick IGO (In:Ga = 65:35 atomic percent) thin films were deposited using RF sputtering method as oxide channel layers, in which oxygen partial pressure was controlled to be 0%, 5%, 10%, and 15% for each device at fixed deposition power of 200 W and fixed working pressure of 5 mtorr. As a matter of convenience for following description, the devices using IGO prepared by different P_{O2} conditions of 0%, 5%, 10%, and 15% were labeled as Ox0, Ox5, Ox10, and Ox15 devices, respectively. In a successive manner, a 9-nm-thick Al_2O_3 was formed by atomic layer deposition (ALD) at 200 °C as a protection layer to prevent any chemical and mechanical damages during the active patterning process [26]. The 176-nm Al_2O_3 gate insulator was then formed by ALD at 150 °C using trimethylaluminium and H_2O as Al and O_2 precursors, respectively. After the formation of metal contact holes, a 150-nm ITO electrode was deposited by dc sputtering method. All the patterning processes were performed by conventional photolithography and wet etching methods. Finally, postannealing processes were performed for Ox0 and other devices at 250 °C and 350 °C, respectively, in a vacuum atmosphere. The device characteristics of fabricated TFTs were evaluated using a semiconductor parameter analyzer (Agilent B1500A) in a dark box. To examine the device instability under the NBIS conditions, the monochromic typical light sources with red (700 nm), green (530 nm), and blue (350 nm) wavelengths were employed and their power densities were confirmed by power meter (Newport, 1918-C). The channel width (W) and length (L) of the evaluated devices were 40 and 20 μm, respectively. To verify the effects of P_{O2}, the IGO thin films with a thickness of 40 nm were separately prepared on Si substrate at different P_{O2} conditions of 0% and 10%. The crystallinity of the prepared IGO thin film was investigated by X-ray diffraction (XRD). The bonding strength and chemical shifts of IGO thin films were measured by X-ray photoelectron spectroscopy (XPS, VG scientific ESCALAB-200R) with depth profiles. The Al–Kα (1486.6 eV) radiation (12.5 kV/20 mA) was used at a scan step of 0.05 eV and the depth profiles of nine steps were obtained using Ar sputtering at 5 keV ion beam power.

III. Results

Fig. 2(a) and (b) shows the crystallinity of IGO thin films prepared with the P_{O2} conditions of 0% and 10% and postannealed at various temperatures ranging from 100 °C to 400 °C at 100 °C intervals. The diffraction patterns were measured using Cu-Kα radiation (40 kV/60 mA) at a scan

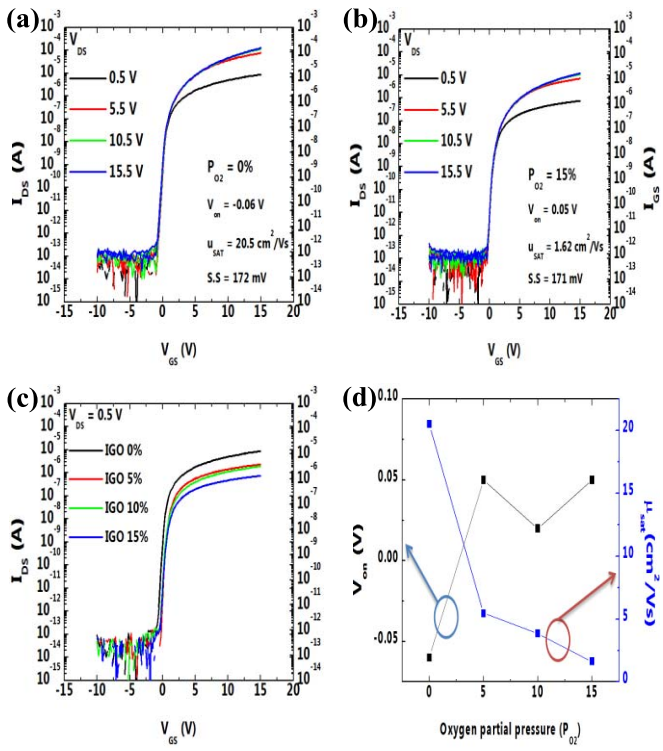

Fig. 3. I_{DS}–V_{GS} transfer characteristics of the fabricated IGO TFTs when the IGO channel layers were prepared with different P_{O2} conditions of (a) 0% and (b) 15%. The channel width and length of measured devices were 40 and 20 μm, respectively. The measurements were performed at V_{DS}'s of 0.5, 5.5, 10.5, and 15.5 V in forward and reverse sweeps of V_{GS}. (c) Transfer curves measured at a V_{DS} of 0.5 V were compared when the P_{O2} during the IGO deposition was varied to 0%, 5%, 10%, and 15%.

rate of 3°/min. Once IGO films were crystallized at given temperatures, detectable peaks can be picked up as follows; In_2O_3 at $2\theta = 30.6°$ and 35.5° corresponding to (222) and (400) planes (JCPDS no. 06-0416), β-Ga_2O_3 at 30.1°, 35.3°, and 37.5° corresponding to (004), (111), and (104) planes, respectively (JCPDS no. 11-370). The only peaks appeared around $2\theta = 32.7°$, which corresponds to (200) plane of Si substrate. The IGO film did not exhibit any marked peaks in XRD patterns even after the annealing at 400 °C. As a result, the IGO films with an In/Ga atomic ratio of 65/35 were confirmed to be amorphous phases and the P_{O2} conditions during the IGO deposition did not have such a significant impact on the crystallinity of the prepared IGO films. These results obtained for the employed composition of IGO were totally different, compared with the fact that the IGO layer with a In/Ga atomic ratio of 90:10 had exhibited typical bixbyite phases even after the annealing in air at 300 °C [15]. The origins of differences in crystallinity after the annealing process at a given temperature between two compositions of 65/35 and 90/10 were not yet clearly figured out.

In advance, the basic transfer characteristics for the fabricated IGO TFTs were confirmed and their device parameters were compared for the devices using IGO channels prepared with different P_{O2} conditions. Fig. 3(a) and (b) shows drain current–gate voltage (I_{DS}–V_{GS}) characteristics of Ox0 and Ox15 devices when the drain voltage (V_{DS}) was varied to be 0.5, 5.5, 10.5, and 15.5 V. Clear transfer behaviors of the TFTs were successfully confirmed for all V_{DS} conditions and the I_{DS}'s were normally scaled with the increase of V_{DS}. Fig. 3(c) compared the I_{DS}–V_{GS} characteristics of all the fabricated IGO TFTs at fixed V_{DS} of 0.5 V, with which the electrical device parameters were calculated for each device, as shown in Fig. 3(d). The field-effect mobility at saturation region (μ_{sat}) and turn-on voltage (V_{ON}), which was defined as the voltage when the I_{DS} launched from the TFT off-state and approached to 10 pA, and SS value for each TFT was obtained to be 20.5 cm^2 V^{-1} s^{-1}, −0.06 V, and 172 mV/decade (Ox0 device), 5.45 cm^2 V^{-1} s^{-1}, 0.05 V, and 170 mV/decade (Ox5 device), 4.46 cm^2 V^{-1} s^{-1}, 0.02 V, and 154 mV/decade (Ox10 device), and 1.62 cm^2 V^{-1} s^{-1}, 0.05 V, and 171 mV/decade (Ox15 device), respectively. From these obtained results, it can be suggested that the carrier concentration (channel conductivity) of the IGO channel layer decreased with increasing P_{O2} during the deposition by reducing the intrinsic defects of oxygen vacancies within the IGO channel. Therefore, although the V_{ON} variations were relatively small compared with the μ_{sat}, the TFTs using the IGO channel prepared with higher P_{O2} exhibited a lower μ_{sat} and a larger V_{ON}, which was in accordance with those reported in previous works [17]. It can be noticeable that the relatively high μ_{sat} of 20.5 cm^2 V^{-1} s^{-1} was obtained for the Ox0 device, even though the In contents composed of the IGO channel layer was suppressed as 65 mol%. For the first evaluation to investigate the stability behaviors, the NBS tests were performed for the fabricated IGO TFTs. A V_{GS} of −20 V was applied to the gate terminal of the TFTs as bias stress for 10^4 s at room temperature. The variations in transfer characteristics during the NBS tests for the Ox0, Ox5, Ox10, and Ox15 devices were investigated (not shown here). Although the V_{ON} was observed to be shifted in a negative direction after the lapse of 10^4 s under NBS, the V_{ON} shifts (ΔV_{ON}) were smaller than 0.1 V for all the devices. The ΔV_{ON}'s of Ox0, Ox5, Ox10, and Ox15 devices were estimated to be ∼0.08, 0.04, 0.05, and 0.06 V, respectively. All devices could be confirmed to show excellent stabilities under the NBS conditions. The positive gate-bias stress (PBS) tests for each device were also investigated (not shown here). The ΔV_{ON}'s of Ox0, Ox5, Ox10, and Ox15 devices were estimated to be ∼0.35, 0.02, 0.16, and 0.19 V, respectively. In general cases, under PBS conditions, the V_{ON} was typically observed to be shifted in a positive direction owing to the electron trapping mechanism [18]. The conventional bottom-gate TFTs are known to be prone to the plasma damages into the gate insulator during the sputtering deposition for the oxide active layers. The damaged interface regions are undesirably subjected to be electron–trapping centers. However, providing that the top-gate-structured oxide TFTs could be well fabricated with excellent interface quality and low density of bulk defects, the negative shifts of the V_{ON} were also feasible [19]. Even for the IGZO TFTs, it was sometimes reported that the ΔV_{ON} under NBS was observed to be smaller than that under PBS [20]–[22]. As for these anomalous negative shifts of V_{ON} during the PBS conditions, various factors may complicatedly affect the resultant properties unlike the simple electron trapping

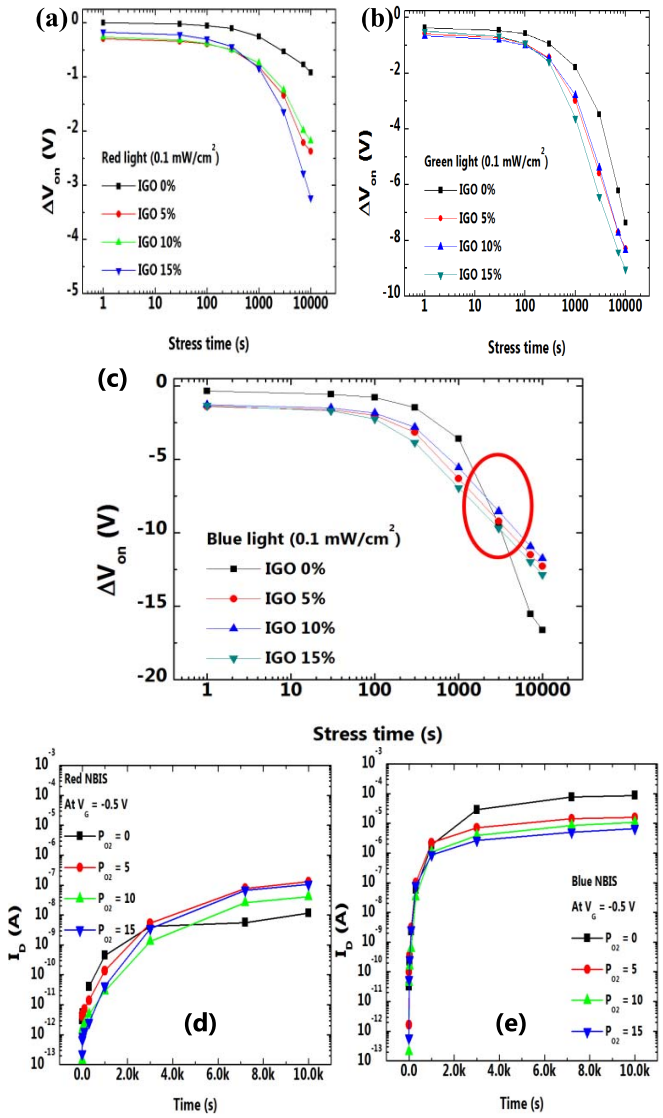

Fig. 4. Variations in V_{on} for the Ox0, Ox5, Ox10, and Ox15 devices as a function of NBIS test time when the illumination light sources were varied to (a) red, (b) green, and (c) blue wavelengths. The bias stress voltage and the power density of light source were −20 V and 0.1 mW/cm^2, respectively. The ΔI_D extracted from the transfer curves of fabricated IGO devices at V_{GS} = −0.5 V during NBIS condition with (d) red and (e) blue light wavelengths.

mechanism. Therefore, the effects of P_{O2} on the negative shifts of V_{ON} during the PBS were difficult to decisively be examined and the variations of ΔV_{ON} among the devices could be regarded as negligible values, which were measured to be as small as 0.35 V. Nevertheless, the negative shift in V_{ON} under the PBS conditions can be supposed to originate from the following two possible reasons: 1) during the deposition of Al_2O_3, H^+ or OH^- species could be slightly incorporated into the IGO channel from the ALD-grown Al_2O_3 layer, which came from the oxygen source of H_2O vapor and 2) the excess holes could be injected from the ITO gate electrode into the ITO/Al_2O_3 interface, which might be resulted from the damaged ITO during the sputtering process. For the specific mechanisms of negative shifts under the PBS conditions, the further experiments will be performed as future works. From

TABLE I
COMPARISONS OF ΔV_{on} FOR THE Ox0, 5, 10, AND 15 DEVICES AFTER NBIS STRESS WITH VARIOUS VISIBLE LIGHT WAVELENGTHS OF RED, GREEN, AND BLUE

Device	ΔV_{on} after NBIS conditions		
	Red NBIS (700 nm)	Green NBIS (530 nm)	Blue NBIS (350 nm)
IGO P_{O2} = 0 %	1.62 V	7.37 V	16.60 V
IGO P_{O2} = 5 %	2.37 V	8.29 V	12.26 V
IGO P_{O2} = 10 %	2.18 V	8.34 V	11.73 V
IGO P_{O2} = 15 %	3.23 V	9.04 V	12.84 V

the discussions on the NBS and PBS instabilities, it could be found that there were no marked differences in the obtained characteristics among the devices. These characteristics were initially confirmed because it was important to guarantee the stable properties under the simple gate-bias stress conditions without illumination. To clearly understand the effects of P_{O2} on the detailed mechanisms for the device instabilities of IGO TFTs, the bias stress under light illumination should be very carefully examined as the next issue.

With the stability behaviors obtained under NBS and PBS tests, the second evaluations to clearly understand the effects of P_{O2} on the detailed mechanisms for the device instabilities of IGO TFTs were performed under NBIS conditions. In these measurements, typical visible light sources with red (1.8 eV, 700 nm), green (2.3 eV, 530 nm), and blue (3.5 eV, 350 nm) wavelengths were employed. Fig. 4(a)–(c) shows the variations in ΔV_{ON}'s of Ox0, Ox5, Ox10, and Ox15 devices as a function of NBIS test time, when V_{GS} of −20 V were continuously applied to the gate terminal for 10^4 s with illuminating visible lights with a power density of 0.1 mW/cm^2. Table I summarized the ΔV_{ON} for each IGO film after the NBIS tests. As shown in Fig. 4(a), the ΔV_{ON}'s of Ox0, Ox5, Ox10, and Ox15 devices after the NBIS test with red light source were estimated to be approximately 1.62, 2.37, 2.18, and 3.23 V, respectively. This result suggests that the V_{ON} instability under NBIS condition using red light source might be degraded with increasing the P_{O2}. This is a definitely different observation compared with that under the simple NBS test, as discussed above. Furthermore, these results can be said to be more-or-less anomalous because it has been generally accepted that higher P_{O2} for the sputtering deposition of oxide-semiconductor may lead to reduce the intrinsic oxygen vacancies working as carrier generators. Jeong *et al.* [23] proposed the thermal annealing process performed at high oxygen pressure as a one of the effective ways to compensate the oxygen vacancy within the IGZO channel layer. The higher oxygen pressure was demonstrated to enable us to obtain a better stability under NBIS stress conditions for IGZO TFTs. The complete opposite tendency in the V_{ON} stability appeared in this paper. Therefore, it can be inferred that the increase in the P_{O2} during the IGO layer deposition did not play roles in electrically compensating the charge carriers (typically oxygen vacancies) but in generating additional defects within the bulk channel layer. It is also interesting to note that the negative shift in V_{ON} of the Ox5, Ox10, and Ox15 devices

drastically increased after the lapse of 300 s. For the case of NBIS test using green light, as shown in Fig. 4(b), the ΔV_{ON}'s of Ox0, Ox5, Ox10, and Ox15 devices were measured to be ~7.37, 8.29, 8.34, and 9.04 V, respectively. Amounts of V_{ON} shifts in a negative direction were larger than those observed for the case of red light illumination for all devices. These phenomena were well explained by higher photon energy of green light. Similarly, the device fabricated with higher P_{O2} condition for IGO channel exhibited a larger shift in V_{ON}. On the other hand, for the case of NBIS test using blue light, as shown in Fig. 4(c), the ΔV_{ON}'s of Ox0, Ox5, Ox10, and Ox15 devices were estimated to be ~16.60, 12.26, 11.73, and 12.84 V, respectively. Larger amounts of V_{ON} shifts in a negative direction could be reasonably accepted for the cases of blue light illumination owing to its much higher photon energy. However, the amount of ΔV_{ON} of the Ox0 device dramatically increased and showed the largest value among the devices. Furthermore, considering that there was not a monotonous increasing or decreasing trend in accordance with P_{O2}, it was expected that there were complex and complicated mechanisms to explain the NBIS instability for the blue light with higher energy. To estimate the changes in carrier generation rates at different light illumination conditions, the differences between the photon-excited current and initial off-current (ΔI_D) were extracted from the transfer curves of the IGO devices after the NBIS tests with red and blue light sources, as shown in Fig. 4(d) and (e). The obtained ΔI_D were significantly increased after the NBIS stress and were dependent on the light wavelength. These results effectively support the fact that the shifts in ΔV_{ON} had a strong dependence on the wavelength of irradiated light source, as shown in Fig. 4(d) and (e). The technical reasons for the acceleration of V_{ON} shift with the increase in P_{O2} under NBIS with red or green light illuminations and for the crossing down in ΔV_{ON} of the Ox0 device under the NBIS with blue light after a lapse of 3000 s will be explained from the XPS profile analysis performed for examining the bonding strength and chemical shift of IGO films prepared with various P_{O2} conditions. To find out the mechanism of instability under NBIS condition, the XPS analyses of IGO layers were carried out. From the NBIS instabilities of IGO TFTs, the tendency of V_{ON} instability could be divided into the two groups with or without oxygen incorporation. Especially, the instability behaviors under NBIS with blue light source were definitely changed between two groups of IGO TFTs. With the results of NBIS conditions, the bonding strengths of IGO thin films deposited with the P_{O2} conditions of 0% and 10% were analyzed as representatives between two groups of stability behaviors. Each specimen was prepared on Si substrate and annealed at 250 °C and 350 °C, respectively. The XPS data for the specimens were compared between before and after the blue light illumination stress with a power density of 1 mW/cm^2 for 3 h as shown in Fig. 5(a). Furthermore, to figure out the variation in binding energy from the interface to the bulk of the IGO layer as well as in chemical shift of species in the IGO layer, the spectroscopy analyses were repeated nine steps with physically etching the layers in film-depth direction. Fig. 5(b)–(d) shows the O 1s narrow scan spectra for two samples, in which the surface,

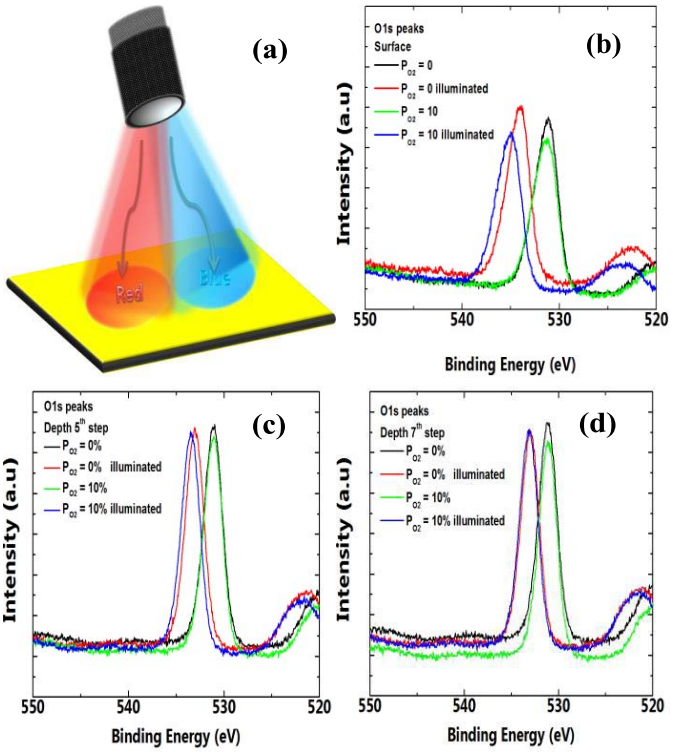

Fig. 5. (a) Schematic diagram of illuminated IGO layer prepared on Si substrate with red and blue light sources and comparisons of O 1s peaks analyzed by XPS for the IGO films deposited on Si substrate with P_{O2} conditions of 0% and 10% between before and after the illumination with blue light source. The power density of illuminated light source and illumination stress time were 1 mW/cm^2 and 3 h, respectively. The spectroscopy analyses were repeated nine steps with physically etching the layers in depth direction. (b) Surface, (c) fifth, and (d) seventh step narrow scan spectra for O 1s peaks were plotted.

fifth, and seventh steps profiles were plotted. These spectra represent the binding energy variation from the surface to the bulk. The peaks obtained at surface were normalized with the C–C bonds of native carbon, located at 284.5 eV (not shown here), as an energy calibration procedure. The binding energies of O 1s for just-annealed IGO layers, which were centered at 531.25 ± 0.20 eV, were related to O^{2-} ions in the oxygen deficient regions [24], [25], as shown in Fig. 5(b)–(d). It should be noticed that the intensity of O 1s peak for the IGO film prepared at the P_{O2} of 10% was higher than that prepared at the P_{O2} of 0%. The atomic percent was estimated by integrating all peaks area of In 3d, Ga 2p, and O 1s of the surface region. The obtained values of surface O 1s peaks for the samples of unilluminated and illuminated 0%, unilluminated and illuminated 10% were 65.4, 65.1, 68.5, and 68.4, respectively. There was no chemical shift and marked variations in peak position between the IGO films prepared with P_{O2} of 0% and 10% before the blue light illumination. For these two just-annealed specimens, remarkable chemical shifts were also not detected as the progress of depth profiles. However, after the IGO films were illuminated with blue light, the O 1s peaks for the IGO films prepared with P_{O2} of 0% and 10% experienced red shifts which means that the XPS peaks shift to the left with higher eV direction from centered peak to 534.5 and 535.03 eV, respectively, when the

TABLE II
COMPARISONS OF ANALYZED PEAKS WITH O 1s ANALYZED BY XPS FOR THE $P_{O2} = 0$ AND 10% THIN FILMS BEFORE AND AFTER BLUE LIGHT ILLUMINATION

Sample	Illumination status	Peak	Depth Step	Analyzed Peaks	Δ eV
	Before illumination	O 1s		531.25 ±.0.20	
IGO 0%	After illumination (Blue light)	O 1s	Surface	534.05	2.80
			5	533.03	2.01
			7	533.02	2.00
IGO 10%	After illumination (Blue light)	O 1s	Surface	535.03	3.78
			5	533.46	2.41
			7	533.11	2.09

depth profiles progressed from the surface, which corresponds to the top interface region, as shown in Fig. 5(b). On the other hand, when the depth profiles progressed to the fifth [Fig. 5(c)] and seventh steps [Fig. 5(d)], which correspond to the bulk and bottom interface regions, respectively, the O 1s peaks for the films with P_{O2} of 0% and 10% also exhibited red shifts to 533.03 and 533.46 eV and to 533.02 and 533.11 eV, respectively. The red shifts in the binding energy of O 1s showed that the number of oxygen vacancy increased by the illumination stress of blue light, which was evidently confirmed from the fact that the degree of red shift was observed to decrease as the progress of depth profiles. Amounts of red shifts in O 1s for the IGO films prepared with P_{O2} of 0% and 10% were summarized as 2.80, 2.01, and 2.00 eV and 3.78, 2.41, and 2.09 eV, respectively, when the depth profiles were progressed from the surface to the fifth and seventh steps, as shown in Table II. As a consequence, the illumination stress and oxygen vacancy generation could be expected to have significant effect at the interface regions. From these results examined by XPS, the tendency of V_{ON} shift for the IGO TFTs under NBIS with red, green and blue light illuminations can be explained as follows. In addition, according to [26], the formation energies of neutral oxygen vacancy in a-IGZO were estimated to be in the range from 2.96 to 5.82 eV, which were calculated by the GGA+U method. Thus, the possibility of oxygen vacancy generation may be much larger for the NBIS test using the blue illumination (3.5 eV, 350 nm) than for the cases using red (1.8 eV, 700 nm) or green (2.3 eV, 530 nm) illuminations. We have to elucidate two typical observations. The first one was that the amounts of ΔV_{ON} increased when the light stress illumination source was changed from red to green and blue for all devices. It is generally accepted for the conventional IGZO TFTs that the negative shifts of V_{ON} can be caused by the photoionized oxygen vacancies generated near the interface between the active channel and gate dielectric layers owing to the hole trapping mechanism [23]. Therefore, larger amounts of ΔV_{on} in the transfer characteristics of each device could be understood as results of the increases in the oxygen vacancies generated by the photon-induced chemical shifts of O 1s bonds. It was clearly confirmed from the XPS analysis that the red shifts of O 1s peaks for the IGO films prepared with P_{O2} of 0% and 10% were accelerated for the light source with higher photon energy (blue illumination) and for the near interface region rather than the bulk.

The second observation was more difficult to understand its origin that the ΔV_{ON} of the Ox0 device started to become larger than those of other devices under the NBIS with only a blue light illumination from the time evolution of 3000 s. This phenomenon was not activated under the NBIS tests using red or green light sources. Here, two competent contributions related to the effects of P_{O2} on the NBIS instabilities of the IGO TFTs could be discussed. One scenario was that the oxygen species incorporated during the process of IGO deposition could work as effective suppressors to decrease the carrier density within the IGO layer. As a result, with increasing the P_{O2} during the process, the number of intrinsic defects inherent in the IGO layers decreased, and hence the electric resistivity of the prepared film increased to a higher value. These discussions were well reflected in the device characteristics shown in Fig. 3(d), in which the μ_{sat} and V_{ON} of the fabricated IGO TFTs showed a decreasing and increasing trends with the increase in incorporated P_{O2}, respectively. In other words, it was found that the Ox0 device included the largest number of intrinsic defects within the IGO channel. On the other hand, another scenario could also be suggested that the ion bombardment caused by incorporated oxygen ions within the oxygen plasma induced some physical damages into the *in situ* deposited IGO film. The chemical bonding strength in the damaged layer was supposed to be weakened and such additional defects as oxygen interstitials might be inserted between the loosely bonded atoms [27], [28]. If this contribution was dominantly accepted for our IGO system, the degree and thickness of the damaged layer, especially near the interface region, could be intensified with increasing the P_{O2} during the IGO deposition. Comprehensively considering these two contributions, the feasible situations could be proposed as follows: 1) for the case of Ox0 device, the IGO active layer deposited without oxygen incorporation had a larger number of intrinsic defects but did not include additionally induced extrinsic defects caused by the physical plasma damages. The bond strength between the atoms was considered to be soundly maintained even after the channel deposition and 2) as the increase in the incorporated oxygen contents (P_{O2}) for the Ox5, Ox10, and Ox15 devices, the strengths of chemical bonds themselves got weak and became sensitive to the externally induced activation energies for the generation of extrinsic defects, while the intrinsic defects such as oxygen vacancies diminished by the oxygen compensation. The amounts of red shifts of O 1s peaks for the IGO film prepared with a P_{O2} of 10% was much larger than those for the IGO film prepared without oxygen (P_{O2} 0%), as previously shown in Fig. 5. As a consequence, when the illumination light source was varied from red to blue with an increase of photon energy, the devices having more severely damaged layer experienced a larger amounts of ΔV_{on} under NBIS conditions. In other

words, the device employing the IGO active layer prepared with a higher P_{O2} showed a larger ΔV_{on} in a negative direction, as shown in Fig. 4(a)–(c). For the normal situations using red and green light sources, the intrinsic defects could not respond to the induced photon energy because they were expected to be located at sufficiently deep states. The plausible typical intrinsic defects of oxygen vacancies could be discovered around the midgap regions within the energy bandgap of IGO, as suggested for the IGZO [29], [30]. Even for the blue illumination with a higher energy, the similar situation could be applied for all devices before the total dose (the product of energy and time) of light stress surmounted a critical value. However, once the total dose eventually surpassed over the critical amount, the intrinsic defects started to be activated as they came out of hibernation and contributed to transport behaviors of electron carries by transition to shallow donor levels. This can be suggested as the most feasible origin why the Ox0 device exhibited the largest ΔV_{ON} among other devices when the blue light illumination was introduced over the time evolution of 3000 s. These results are extremely interesting to clearly describe the NBIS instabilities of the proposed IGO TFTs. It was found that the defect types (intrinsic or extrinsic) and amounts could be varied with the different P_{O2} conditions during the IGO deposition using sputtering method. Therefore, according to the defect structures of IGO active channels and stress conditions in environments, a dominant contribution could be separately defined between two mechanisms discussed above. Furthermore, it was also suggested that the defect structures in the IGO semiconducting films and their responses to the bias/light stresses could be concluded to be different from those for the conventionally discussed IGZO.

As discussed above, the different P_{O2} conditions during the IGO deposition process could have effects on the types and amounts of structural defects inside the IGO channel, and hence the stability characteristics under the NBIS with typical visible light sources such as red, green, and blue illuminations could be completely different, depending on the photon energy and induced time of illuminated light stress. Therefore, the P_{O2} should be very carefully controlled as one of the most important process parameters to realize highly stable IGO TFTs. Moreover, to secure the IGO TFT having both performances of high mobility and excellent stability, more extensive researches to optimize the IGO channel composition and corresponding deposition conditions should be performed as future works.

IV. Conclusion

An IGO thin film with an In/Ga atomic ratio of 65/35 was proposed as a promising material for an active channel layer of the oxide-semiconductor TFTs featured to have both performances of high mobility and excellent stability. As a main purpose of this paper, the effects of the IGO deposition conditions of oxygen partial pressure during the sputtering process were systematically investigated to elucidate the mechanisms for the NBIS instability characteristics of the IGO TFTs under red, green, and blue light illuminations. All the prepared IGO films were confirmed to be amorphous phases irrespective of P_{O2}. The device parameters such as μ_{sat} and V_{ON} were found to be sensitively changed with the variations in P_{O2}. The incorporated oxygen during the sputtering deposition was found to play an important role of reducing the carrier concentration originated from the intrinsic defects, such as oxygen vacancies, within the IGO channel. All the fabricated IGO TFTs also showed excellent stability characteristics under NBS or PBS conditions. However, the combination of illumination stress under typical visible lights completely changed the situations. For the cases of red and green illuminations, the amounts of ΔV_{on} monotonically increased with the increase in the incorporated amounts of oxygen and with the time evolution. On the other hand, for the blue illumination with higher photon energy, the increase in ΔV_{ON} for the Ox0 device with the lapse of stress time was dramatically accelerated from the stress time of 3000 s and eventually exhibited the maximum values among the devices. To investigate these interesting phenomena, the XPS analyses were compared between the IGO thin films prepared with P_{O2} of 0% and 10% before and after the blue light illumination, in which the O 1s peak was analyzed in a depth direction with physically etching the film with nine steps. With the XPS results, it was confirmed that the red shifts of O 1s peak for the IGO films prepared with different P_{O2} conditions showed an increasing trend with the increase in photon energy of the illuminated light source and with the progress in depth from the interface region to the bulk. Furthermore, the amounts of red shifts of all peaks for the IGO film prepared with a P_{O2} of 10% were much larger than those for the IGO prepared without oxygen. All these observations were explained by the fact that the defect types (intrinsic or extrinsic) and amounts inherent within the oxide semiconducting channel could be affected with the different P_{O2} conditions during the IGO deposition. In this paper, the instability mechanisms of IGO TFTs under the NBIS conditions using visible light sources were successfully demonstrated by means of careful analysis of XPS depth profiles for the IGO channel layers. It was concluded that the P_{O2} during the sputtering deposition of IGO channel layers for the TFT applications should be carefully controlled as one of the most important process factors for realizing highly stable IGO TFTs with high mobility. We believe that these investigations on the feasible mechanism to understand the NBIS instabilities of the IGO TFT can be a significantly valuable insight for the developments of oxide TFT-related technologies.

References

[1] K. Nomura, H. Ohta, A. Takagi, T. Kamiya, M. Hirano, and H. Hosono, "Room-temperature fabrication of transparent flexible thin-film transistors using amorphous oxide semiconductors," *Nature*, vol. 432, pp. 488–492, Jul. 2004.

[2] J. F. Wager, "Transparent electronics," *Science*, vol. 300, pp. 1245–1246, May 2003.

[3] M. K. Ryu, S. Yang, S. H. Ko Park, C. S. Hwang, and J. K. Jeong, "Impact of Sn/Zn ratio on the gate bias and temperature-induced instability of Zn–In–Sn–O thin film transistors," *Appl. Phys. Lett.*, vol. 95, no. 17, pp. 173508-1–173508-3, Oct. 2009.

[4] J. K. Jeong, H. W. Yang, J. H. Jeong, Y. G. Mo, and H. D. Kim, "Origin of threshold voltage instability in indium-gallium-zinc oxide thin film transistors," *Appl. Phys. Lett.*, vol. 93, no. 12, pp. 123508-1–123508-3, Jul. 2008.

[5] J. S. Park, J. K. Jeong, H. J. Chung, Y. G. Mo, and H. D. Kim, "Electronic transport properties of amorphous indium-gallium-zinc oxide semiconductor upon exposure to water," *Appl. Phys. Lett.*, vol. 92, no. 7, pp. 072104-1–072104-3, Feb. 2008.

[6] J. S. Kachirayil, K. J. Madambi, K. Nomura, T. Kamiya, and H. Hosono, "Optical and carrier transport properties of cosputtered Zn–In–Sn–O films and their applications to TFTs," *J. Electrochem. Soc.*, vol. 155, pp. H390–H395, Apr. 2008.

[7] S. Yang, D. H. Cho, M. K. Ryu, S. H. Ko Park, C. S. Hwang, J. Jang, *et al.*, "High-performance Al–Sn–Zn–In–O thin-film transistors: Impact of passivation layer on device stability," *IEEE Electron Device Lett.*, vol. 31, no. 2, pp. 144–146, Feb. 2010.

[8] J. H. Noh, S. Y. Ryu, S. J. Jo, C. S. Kim, S.-W. Sohn, P. D. Rack, *et al.*, "Indium oxide thin-film transistors fabricated by RF sputtering at room temperature," *IEEE Electron Device Lett.*, vol. 31, no. 6, pp. 567–569, Jun. 2012.

[9] N. Itagaki, T. Iwasaki, H. Kumomi, T. Den, K. Nomura, T. Kamiya, *et al.*, "Zn–In–O based thin-film transistors: Compositional dependence," *Phys. Status Solidi (A)* vol. 205, no. 8, pp. 1915–1919, Aug. 2008.

[10] T. Iwasaki, N. Itagaki, T. Den, H. Kumomi, K. Nomura, T. Kamiya, *et al.*, "Combinatorial approach to thin-film transistors using multicomponent semiconductor channels: An application to amorphous oxide semiconductors in In–Ga–Zn–O system," *Appl. Phys. Lett.*, vol. 90, no. 24, pp. 242114-1–242114-3, Jun. 2007.

[11] C. J. Kim, S. W. Kim, J. H. Lee, J. S. Park, S. I. Kim, J. C. Park, *et al.*, "Amorphous hafnium-indium-zinc oxide semiconductor thin film transistors," *Appl. Phys. Lett.*, vol. 95, no. 25, pp. 252103-1–252103-3, Dec. 2009.

[12] E. G. Chung, Y. S. Chun, and S. Y. Lee, "Amorphous silicon–indium–zinc oxide semiconductor thin film transistors processed below 150 °C," *Appl. Phys. Lett.*, vol. 97, pp. 102102-1–102102-3, Sep. 2010.

[13] G. Gonçalves, P. Barquinha, L. Pereira, N. Franco, E. Alves, R. Martins, *et al.*, "High mobility a-IGO films produced at room temperature and their application in TFTs," *Electrochem. Solid-State Lett.*, vol. 13, pp. H20–H22, Nov. 2010.

[14] T. Arai and Y. Shiraishi, "Manufacturing issues for oxide TFT technologies for large-sized AMOLED displays," in *SID Int. Symp. Dig. Tech. Papers*, vol. 43. Oct. 2012, pp. 756–759.

[15] P. Barquinha, A. Pimentel, A. Marques, L. Pereira, R. Martins, and E. Fortunato, "Influence of the semiconductor thickness on the electrical properties of transparent TFTs based on indium zinc oxide," *J. Non-Cryst. Solids*, vol. 352, nos. 9–20, pp. 1749–1752, Jun. 2006.

[16] S. H. Ko Park, D. H. Cho, C. S. Hwang, S. Yang, M. K. Ryu, C. W. Byun, *et al.*, "Channel protection layer effect on the performance of oxide TFTs," *ETRI J.*, vol. 31, no. 6, pp. 653–659, Dec. 2009.

[17] H. Q. Chiang, B. R. McFarlane, D. Hong, R. E. Presley, and J. F. Wager, "Processing effects on the stability of amorphous indium gallium zinc oxide thin-film transistors," *J. Non-Cryst. Solids*, vol. 354, pp. 2826–2830, May 2008.

[18] J. K. Jeong, "The status and perspectives of metal oxide thin-film transistors for active matrix flexible displays," *Semicond. Sci. Technol.*, vol. 26, no. 3, pp. 034008-1–034008-10, Feb. 2011.

[19] M. K. Ryu, S. H. Ko Park, C. S. Hwang, and S. M. Yoon, "Comparative studies on electrical bias temperature instabilities of In–Ga–Zn–O thin film transistors with different device configurations," *Solid-State Electron.*, vol. 89, pp. 171–176, Nov. 2013.

[20] K. H. Ji, J. I. Kim, Y. G. Mo, J. H. Jeong, S. Yang, C. S. Hwang, *et al.*, "Comparative study on light-induced bias stress instability of IGZO transistors with SiN_x and SiO_2 gate dielectrics," *IEEE Electron Device Lett.*, vol. 31, no. 12, pp. 1404–1406, Dec. 2010.

[21] J. Y. Bak, S. Yang, M. K. Ryu, S. H. Ko Park, C. S. Hwang, and S. M. Yoon, "Effect of the electrode materials on the drain-bias stress instabilities of In–Ga–Zn–O thin-film transistors," *ACS Appl. Mater. Inter.*, vol. 4, no. 10, pp. 5369–5374, Sep. 2012.

[22] W.-S. Cheong, J.-M. Lee, J.-H. Lee, S.-H. Ko Park, S. M. Yoon, C.-W. Byun, *et al.*, "Effects of interfacial dielectric layers on the electrical performance of top-gate In–Ga–Zn–Oxide thin-film transistors," *ETRI J.*, vol. 31, pp. 660–666, Dec. 2009.

[23] K. H. Ji, J. I. Kim, H. Y. Jung, S. Y. Park, R. Choi, U. K. Kim, *et al.*, "Effect of high-pressure oxygen annealing on negative bias illumination stress-induced instability of InGaZnO thin film transistors," *Appl. Phys. Lett.*, vol. 98, no. 10, pp. 103509-1–103509-3, Mar. 2011.

[24] J. C. C. Fan and J. B. Goodenough, "X-ray photoemission spectroscopy studies of Sn-doped indium-oxide films," *J. Appl. Phys.*, vol. 48, pp. 3524–3531, Aug. 1977.

[25] S. Major, S. Kumar, M. Bhatnagar, and K. L. Chopra, "Effect of hydrogen plasma treatment on transparent conducting oxides," *Appl. Phys. Lett.*, vol. 49, pp. 394–396, Aug. 1986.

[26] H.-K. Noh, K. J. Chang, B. Ryu, and W.-J. Lee, "Electronic structure of oxygen-vacancy defects in amorphous In–Ga–Zn–O semiconductors," *Phys. Rev. B*, vol. 84, no. 14, pp. 115205-1–115205-8, Sep. 2011.

[27] P. Erhart, A. Klein, and K. Albe, "First-principles study of intrinsic point defects in ZnO: Role of band structure, volume relaxation, and finite-size effects," *Phys. Rev. B*, vol. 72, pp. 082513-1–082513-6, Aug. 2005.

[28] D. C. Look and J. W. Hemsky, "Residual native shallow donor in ZnO," *Phys. Rev. Lett.*, vol. 82, no. 12, pp. 2552–2555, Mar. 1999.

[29] K. Nomura, T. Kamiya, and H. Hosono, "Interface and bulk effects for bias–light-illumination instability in amorphous-In–Ga–Zn–O thin-film transistors," *J. Soc. Inf. Display*, vol. 18, no. 10, pp. 789–795, Oct. 2010.

[30] X. Huang, C. Wu, H. Lu, F. Ren, Q. Xu, H. Ou, *et al.*, "Electrical instability of amorphous indium-gallium-zinc oxide thin film transistors under monochromatic light illumination," *Appl. Phys. Lett.*, vol. 100, no. 24, pp. 243505-1–243505-4, Jun. 2012.

Jun Yong Bak was born in Busan, Korea, in 1984. He received the B.S. and M.S. degrees from the Department of Nano Semiconductor Engieering, Korea Maritime and Ocean University, Busan, in 2009 and 2011, respectively. He is currently pursuing the Ph.D. degree with Kyung Hee University, Seoul, Korea.

Shinhyuk Yang, photograph and biography not available at the time of publication.

Ho-Jun Ryu, photograph and biography not available at the time of publication.

Sang Hee Ko Park, photograph and biography not available at the time of publication.

Chi Sun Hwang, photograph and biography not available at the time of publication.

Sung Min Yoon received the B.S. degree from the Department of Inorganic Material Engineering, Seoul National University, Seoul, in 1995, and the M.S. and Ph.D. degrees from the Department of Applied Electronics, Tokyo Institute of Technology, Tokyo, Japan, in 1997 and 2000, respectively.

He is currently an Associate Professor with Kyung Hee University, Seoul.